SMTCT
Society of Land Measurements and Cadastre from Transylvania

Zerrouk L *et al.* (2024)
**Notulae Scientia Biologicae**
Volume 16, Issue 2, Article number 11823
DOI:10.15835/nsb16211823
Research Article

NSB
Notulae Scientia Biologicae

# Synthesis, characterization, cyclic voltammetry, and molecular docking studies of the antioxidant activities of superoxide anion radicals towards meso-tetramethophenyl-porphyrin and meso-tetrabiphenyl-porphyrin

Lalmi ZERROUK[1,3], Lazhar BECHKI[1,4], Elhafnaoui LANEZ[2,3]*, Touhami LANEZ[3]

[1]*Kasdi Merbah University, Faculty of Mathematics and Material Sciences, Department of Chemistry, 30000 Ouargla, Algeria; l_zerrouk@yahoo.fr; lbechki1@gmail.com*
[2]*University of Eloued, Faculty of Biology, Department of Cellular and Molecular Biology, 39000 Eloued, Algeria; lanez-elhafnaoui@univ-eloued.dz (*corresponding author)*
[3]*University of Eloued, VTRS Laboratory, Department of Chemistry, Faculty of Exact Sciences, B.P.789, 39000 Eloued, Algeria; lanezt@gmail.com*
[4]*Kasdi Merbah University, VPRS Laboratory, Department of Chemistry, Faculty of Mathematics and Material Sciences, 30000 Ouargla, Algeria*

## Abstract

The investigation employed cyclic voltammetry (CV) assays to assess the scavenging efficacy of two recently developed compounds, namely meso-tetramethophenyl-porphyrin $TPPH_2$(o-methyl) and meso-tetrabiphenyl-porphyrin ($TbiPPH_2$), against the superoxide anion radical ( $O_2^{\cdot-}$). The $IC_{50}$ values derived from the CV assays indicated significant scavenging activity for both compounds, with $TbPPH_2$ exhibiting superior potency (85.79 ± 0.11 μg $ml^{-1}$) compared to the standard antioxidant alpha-tocopherol (353.27 ± 3.21 μg $ml^{-1}$). Additionally, molecular docking simulations elucidated the interaction of the investigated compounds with specific amino acid residues of glutathione reductase through hydrogen bonding and hydrophobic interactions. The in vitro and in silico results were concordant, highlighting $TbiPPH_2$ as the least active compound against glutathione reductase, boasting the highest inhibitory concentration of 0.63 μM and the lowest docking score of -35.36 kJ $mol^{-1}$, thus positioning it as a promising candidate for antioxidant applications.

***Keywords:*** antioxidant activity coefficient; binding free energy; cyclic voltammetry; homogeneous rate constant; molecular docking study; porphyrin

## Introduction

Meso-tetramethophenyl-porphyrin and meso-tetrabiphenyl-porphyrin represent macrocyclic aromatic compounds characterized by an 18π electron structure, composed of four pyrrole subunits interconnected through methine bridges. These compounds exhibit noteworthy electron mobility within the ring, rendering

*Received: 10 Dec 2023. Received in revised form: 22 Mar 2024. Accepted: 22 Apr 2024. Published online: 13 May 2024.*
From Volume 13, Issue 1, 2021, Notulae Scientia Biologicae journal uses article numbers in place of the traditional method of continuous pagination through the volume. The journal will continue to appear quarterly, as before, with four annual numbers.

them suitable for diverse applications (Meraghni *et al.*, 2023), including electrochemistry and catalysis (Zuriaga-Monroy *et al.*, 2016), photomedicine (Boutarfaia *et al.*, 2020), and photosynthesis (Zaiz *et al.*, 2012). The nitrogen atoms in these compounds possess the ability to engage in reactions with metal ions, forming stable metalloporphyrin complexes, with transition metal ion complexes being the most extensively studied (Thompson *et al.*, 2018).

The superoxide anion free radical, denoted as $O_2^{\cdot-}$, remains a prominent target for evaluating the antioxidant activity of various biological solutions, including extracts and antioxidant compounds (Lanez *et al.*, 2017; Lanez *et al.*, 2015). This assay, commonly employed to assess antioxidant efficacy, measures the reduction in the anodic peak current density of the redox couple following the introduction of the antioxidant $O_2/O_2^{\cdot-}$. Notably, the existing literature predominantly focuses on the antioxidant activity of potential compounds, expressed as IC50, while neglecting the binding parameters governing the interaction between the free radical $O_2^{\cdot-}$ and antioxidant compounds (Ahmed *et al.*, 2012a,b).

The stable radical species, the superoxide anion free radical, is generated through the one-electron reduction of molecular oxygen or the one-electron oxidation of hydrogen peroxide. Its reactivity contributes to critical roles in various chemical and biological systems, particularly within biological systems during normal metabolic processes. The superoxide anion free radical's presence can lead to deleterious effects on cellular components, including aging, oxidative stress, cancer, and lipid peroxidation, as documented in numerous studies (Giustarini *et al.*, 2009; Sen *et al.*, 2010; Ighodaro *et al.*, 2018).

Glutathione, a tripeptide protein endogenously produced, plays a vital intracellular antioxidant role by neutralizing reactive oxygen species and scavenging various oxygen radicals (Yao *et al.*, 2021). The enzyme glutathione reductase (GR) is pivotal in converting the oxidized form of glutathione disulfide (GSSG) to the reduced glutathione form (GSH). Preserving a low GSSG/GSH ratio helps maintain intracellular redox balance, aiding in the elimination of free radicals and reactive oxygen species (Patra *et al.*, 2017). Therefore, inhibiting glutathione reductase results in decreased GSH, increased GSSG, and a higher GSSG/GSH ratio. Investigating the inhibition of glutathione reductase by potential antioxidant compounds assists in identifying effective antioxidant candidates, with an ideal candidate exhibiting a lesser inhibitory effect (Kedadra *et al.*, 2022).

This study presents the synthesis, binding parameters, and scavenging activity against $O_2^{\cdot-}$ of meso-tetramethophenyl-porphyrin ($TPPH_2$(o-methyl)) and meso-tetrabiphenyl-porphyrin ($TbiPPH_2$) through cyclic voltammetry assays. Furthermore, molecular docking was employed to elucidate the inhibition and binding preferences of the most potent compound with glutathione reductase.

## Materials and Methods

### *Chemical*

N,N-Dimethylformamide (DMF), procured in HPLC-grade quality from Sigma-Aldrich, served as the solvent in electrochemical assays. Tetrabutylammonium tetrafluoroborate ($Bu_4NBF_4$), obtained in electrochemical grade (99%) from Sigma-Aldrich, was utilized as the supporting electrolyte, maintaining a concentration of 0.1 M. Molecular oxygen, sourced from a research-grade cylinder (99.99%) provided by Linde gaz Algérie, was employed in the experiments. α-tocopherol ($C_{29}H_{50}O_2$, MW = 430.71), acquired at a purity of 97% from Alfa Aesar, was utilized without further purification in the study.

### *Synthesis*

The synthesis of $TPPH_2$(o-methyl) (Figure 1a) and $TbPPH_2$ (Figure 1b) involved the reaction of pyrrole in propionic acid (500 mL) with 2-methylbenzaldehyde (35.5 mL, 340 mmol) and biphenyl-4-carbaldehydee (30.5 mL, 300 mmol), respectively. The colourless mixture was stirred at room temperature until

complete dissolution of the aldehyde, followed by heating at 50 °C. A solution of distilled pyrrole (25 mL, 360 mmol) in propionic acid (30 mL) was then added dropwise over approximately 10 minutes, and the reaction mixture was refluxed for 30 minutes. Subsequently, the mixture was allowed to cool to room temperature. The resulting dark suspension was filtered, washed with 50 mL methanol/water (1:1), and further washed with methanol until the filtrate clarified. The obtained purple solid was then vacuum-dried, yielding 10.6 g of meso-tetraphenyl-porphyrin (8.2%) and 6.6 g of meso-tetrabiphenyl-porphyrin (8%).

**$TPPH_2$(o-methyl):** $\lambda_{max}$ ($CH_2Cl_2$)/nm: 417, 514 (log M 5.88 and 4.43).

$^1$H-NMR (200 MHz, $CDCl_3$): δ (ppm): -2.10 (s, 2H, NH), 3.1 (s, 12H, $CH_3$), 8.2 (d, 8H, benzene), 8.4 (d, 8H, benzene), 9.1 (d, 8H, β-pyrrole).

MS: m/z, 671($M^+$)

**$TbPPH_2$:** $\lambda_{max}$ ($CH_2Cl_2$)/nm: 417, 514 (log M 6.98 and 5.63).

$^1$H-NMR (200 MHz, CDCl3): δ (ppm): -3.10 (s, 2H, NH), 8.2 (t, 4H, benzene), 8.4 (t, 8H, benzene), 9.1 (d, 8H, benzene), 10 (d, 8H, benzene), 5.7 (d, 8H, benzene), 9.1 (d, 8H, β-pyrrole).

MS: m/z, 919.50($M^+$)

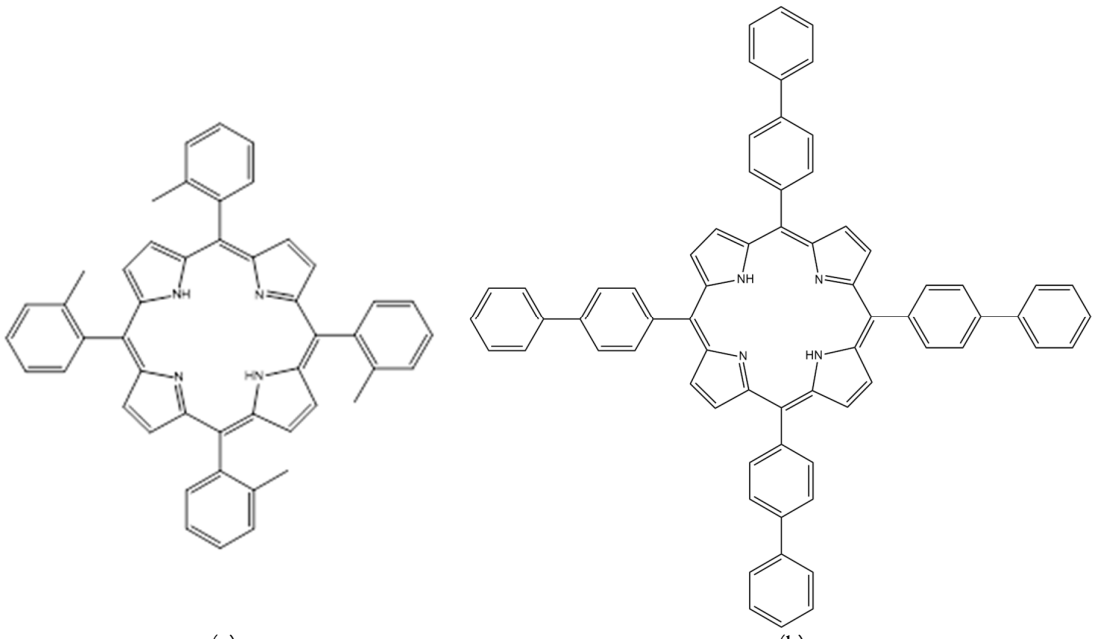


(a) (b)

**Figure 1**. Structure of: $TPPH_2$(o-methyl) (a) and $TbPPH_2$ (b)

*Instrumentation and software*

Cyclic voltammetry experiments were conducted using a PGZ301 potentiostat (Radiometer Analytical SAS) and a voltametric cell with a volumetric capacity of 25 mL, comprising three electrodes: a glassy carbon working electrode with an area of 0.013 $cm^2$, a Pt wire counter electrode, and a $Hg/Hg_2Cl_2$ reference electrode (3.0 M KCl). Prior to each experiment, the solutions were saturated with high-purity commercial oxygen for 15 minutes.

$^1$H NMR spectra were acquired on a Bruker Advance 400 spectrometer operating at 400.155 MHz, utilizing deuterated chloroform at 7.26 ppm as an internal reference.

Molecular docking simulations were executed using AutoDock 4.2 docking software (Morris *et al.*, 1998), implemented on a Pentium 2.7 GHz processor with 8 GB RAM, operating on a microcomputer with Windows 8.

*In vitro antioxidant assay*

In the *in vitro* antioxidant assay, a precise electrochemical setup was utilized, consisting of a 25 mL three-electrode cell filled with 15 ml DMF solution and 0. M $Bu_4NBF_4$ as the supporting electrolyte. The cell was saturated with oxygen for 15 minutes before recording cyclic voltammograms within a defined potential range. Glassy carbon electrodes were used, and prior to each run, they were meticulously polished for consistent results. The experiments were repeated three times to ensure reliability and the ability of the test sample to quench $O_2^{\cdot-}$ radicals (% Inhibition of $O_2^{\cdot-}$ ) was determined from equation (1) (Brand-Williams *et al.*, 1995; Antolovich *et al.*, 2002; P, 2004; Lanez *et al.*, 2019a).

$$\%\ O_2^{\cdot-}\ \text{radical scavenging activity} = \frac{i_0 - i}{i_0} \times 100 \qquad (1)$$

Where $i_0$ and i are the anodic peak current densities of the superoxide anion radical in the absence and presence of the potential antioxidant compound, respectively.

*Docking setup*

Ligands preparation

In order to preform molecular docking studies, firstly, a fully optimized three-dimensional structure of the title compounds was obtained using density functional theory (DFT) without imposing any symmetry constraints; calculations were realized with the Gaussian 09 package (Frisch *et al.*, 2009). The exchange functional of Becke and the correlation functional of Lee, Yang and Parr (B3LYP) were employed with LanL2DZ basis set (Frisch *et al.*, 1988). The optimized structures of the compounds are depicted in Figure 2.

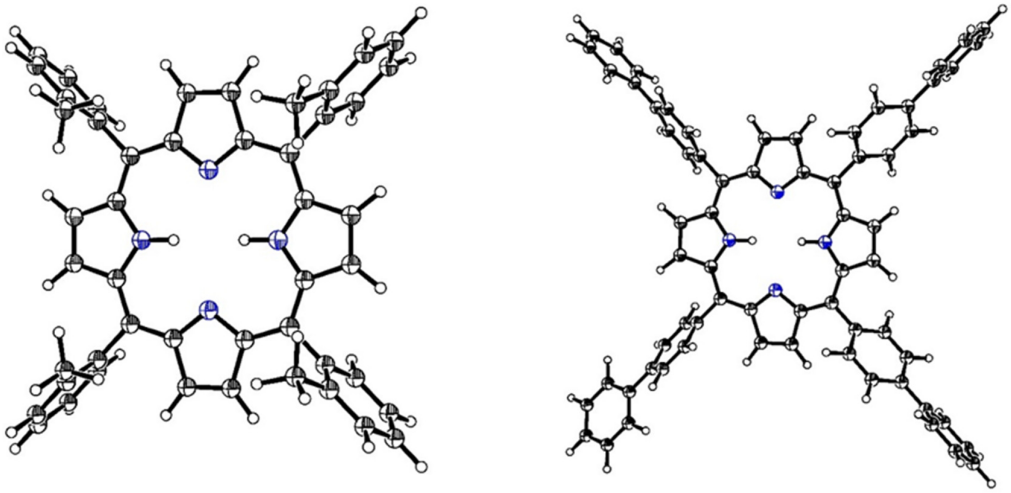

(a) (b)

**Figure 2.** 3D conformation of ligands: (a) $TPPH_2$(o-methyl) and (b) $TbPPH_2$, (ORTEP View 03, V1.08); thermal ellipsoids are plotted at the 50% probability level

The two-dimensional (2D) structure of the standard alpha-tocopherol was downloaded from PubChem database (Kim *et al.*, 2016) (*https://pubchem.ncbi.nlm.nih.gov/*), converted to three-dimensional (3D) structure and thereafter prepared for docking, the 3D structure of alpha-tocopherol is presented in Figure 3.

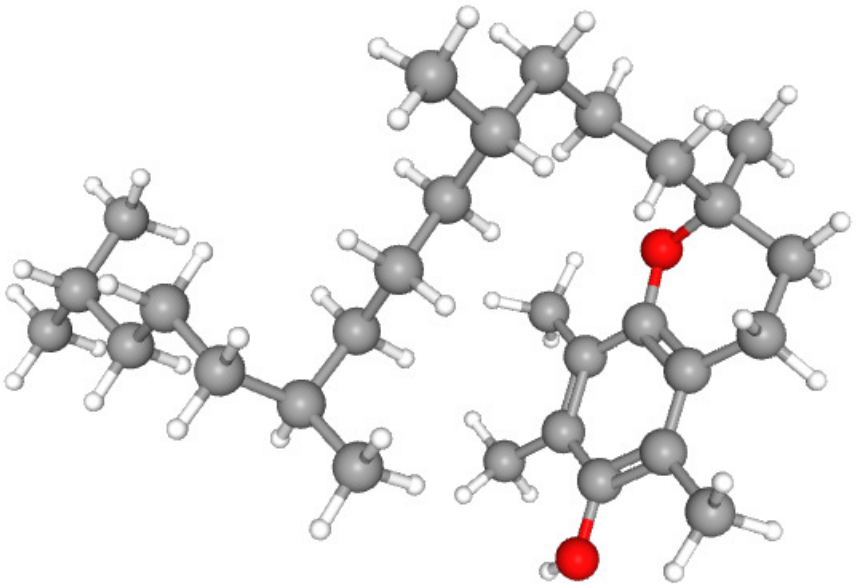

**Figure 3.** 3D conformation of ligand alpha-tocopherol downloaded from PubChem database (CID 14985)

Receptor preparation

The glutathione reductase receptor (GR) with Protein Data Bank ID 1GRE was selected as the target for this investigation. The three-dimensional structure of the target receptor was retrieved from the RCSB Protein Data Bank (*https://www.rcsb.org/structure/1GRE*) (Karplus *et al.*, 1989), as detailed in Table 1. Initial preparation of the receptor involved using AutoDock Tools (ADT) (Morris *et al.*, 2008). This preparation entailed the removal of all water molecules and cofactors to acquire the raw protein structure. Subsequently, the active site was defined, and polar hydrogens were added, followed by the assignment of Kollman charges.

**Table 1.** Target receptor information chosen for docking studies (Karplus *et al.*, 1989)

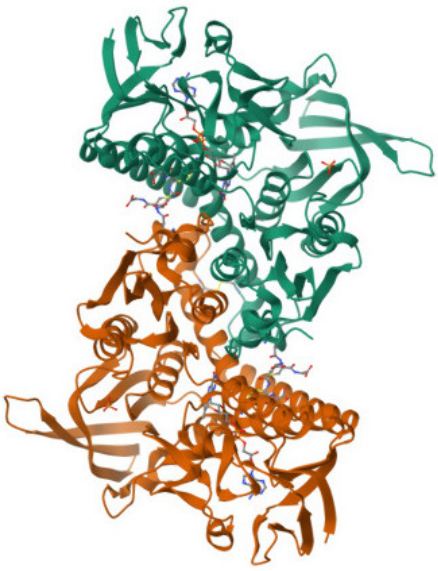

| Human glutathione reductase | |
|---|---|
| PDB ID | 1GRE |
| Resolution (Å) | 2.00 |
| Mutation | No |
| R-Value | 0.155 |
| Space Group | B 1 1 2 |
| Chains | A |
| Organism | *Homo sapiens* |

Molecular docking studies

To investigate the binding affinities between the glutathione reductase receptor (GR) and the examined ligands, an automated docking procedure was executed utilizing AutoDock 4 (Morris *et al.*, 2009). The grid map delineating the protein binding site for docking was computed with the assistance of AutoGrid. For glutathione reductase, a grid size of 50×50×50 Å points in each dimension, with a spacing of 0.5 Å and coordinates X=62.68, Y=50.07, and Z=18.34, was established. All potential torsions of ligand molecules for the docking algorithm were incorporated via the autotors utility in AutoDock Tools.

Docking was conducted with the following parameters: 15 docking trials, a population size of 150, a maximum of 250,000 energy evaluations, a maximum of 27,000 generations, a mutation rate of 0.02, a crossover rate of 0.8, an elitism value of 1, and other parameters set to default values. Subsequently, the docking pose with the superior binding affinity score (kcal/mol) was designated as the primary orientation for each ligand against GR. The most favourable poses with the lowest docking energy (Lanez *et al.*, 2019b; Khennoufa *et al.*, 2021; Laraoui *et al.*, 2023) were chosen and employed in the analysis of docking binding interactions. Visualization of the docking interactions was performed using the PLIP webserver (Protein-Ligand Interaction Profiler) (Salentin *et al.*, 2015; Li *et al.*, 2019).

*Statistical analysis*

Experimental values are given as means ± standard error of three replicates for antioxidant activity. Statistical calculations were carried out by Microsoft Excel software.

## Results and Discussion

*Free radical scavenging activities study*

In this investigation, the scavenging activity against $O_2^{\cdot-}$ radicals were utilized to assess the antioxidant potential of $TPPH_2$(o-methyl) and $TbPPH_2$. Kinetic curves and $IC_{50}$ values were generated by plotting the $O_2^{\cdot-}$ radical scavenging activity against varying concentrations of the compounds, specifically (6.63, 13.14, 19.51, 25.77, 37.92, 43.83, 49.63, 55.32, and 60.91 µg/mL) for $TPPH_2$(o-methyl) and (9.09, 18, 26.74, 35.31, 51.96, 60.06, 68, 75.79, and 83.45 µg $mL^{-1}$) for $TbPPH_2$. The antioxidant capacity of both compounds was quantified in terms of $IC_{50}$, representing the concentration (µg $mL^{-1}$) at which the potential antioxidant inhibits the formation of $O_2^{\cdot-}$ radicals by 50%. All measurements were conducted in triplicate, and the graph was plotted using the averages of three observations.

The linear calibration graph equations within the studied concentration range for $TPPH_2$(o-methyl), $TbPPH_2$, and α-tocopherol are summarized in Table 2, where 'y' denotes the value of the anodic peak current density of $O_2^{\cdot-}$, and 'x' represents the sample concentrations expressed in µg $mL^{-1}$.

Both $TPPH_2$(o-methyl) and $TbPPH_2$ exhibit significant $O_2^{\cdot-}$ radicals scavenging activities, with the antioxidant activity of $TPPH_2$(o-methyl) nearly equivalent to that of $TbPPH_2$ (Table 2). Notably, the antioxidant activity of both studied compounds is four times higher than that of the standard antioxidant α-tocopherol.

*Antioxidant activity coefficient*

The antioxidant activity coefficient ($K_{aac}$) is defined as the ratio of the peak anodic current density values of $O_2^{\cdot-}$ in the presence and absence of the studied antioxidant compounds. This coefficient serves as a measure of the relative superoxide scavenging activity (Korotkova *et al.*, 2003), indicating the compound's efficacy in scavenging superoxide radicals. The calculation of $K_{aac}$ is performed using Equation (2):

$$K_{aac} = \frac{\Delta i}{(i_0 - i_{res})} \cdot \frac{1}{\Delta C} \quad (2)$$

Here, Δi represents the variation in anodic peak current density resulting from the addition of the antioxidant compound, $i_0$ is the anodic peak current density in the absence of the studied antioxidant compound, $i_{res}$ is the residual current density of oxygen in the system, and ΔC is the variation in the concentration of the studied antioxidant compound in mol $L^{-1}$.

It is essential to note that Equation (2) is applicable only at low concentrations of the studied antioxidant compound, corresponding to the linear change region. The obtained values of $K_{aac}$ are presented in Table 2.

**Table 2.** $IC_{50}$ and $K_{aac}$ values obtained using $O_2^{\cdot-}$ radicals scavenging activity

| Compound | Equation | $R^2$ values | $IC_{50}$ (µg $mL^{-1}$) | $K_{aac}$ |
|---|---|---|---|---|
| $TPPH_2$(o-methyl) | y = 0.556x + 1.849 | 0.997 | 86.59 ± 0.06 | 3,736.76 ± 4.81 |
| $TbPPH_2$ | y = 0.505x + 6.679 | 0.994 | 85.79 ± 0.11 | 4.813.45 ± 5.23 |
| α-Tocopherol | y = 0.141x + 0.149 | 0.950 | 353.27 ± 3.21 | 1.929.37 ± 3.88 |

The calculated $K_{aac}$ values for $TPPH_2$(o-methyl) and $TbPPH_2$ were determined to be 3,736.76 ± 4.81 and 4,813.45 ± 5.23, respectively. These values are notably higher than that of α-tocopherol (1,929.37 ± 3.88). The results indicate that both $TPPH_2$(o-methyl) and $TbPPH_2$ exhibit a significantly stronger relative superoxide scavenging activity compared to α-tocopherol.

*Voltammetric studies of $O_2^{\cdot-}$_$TPPH_2$(o-methyl) and $O_2^{\cdot-}$_$TbPPH_2$ interaction*

Figure 4 illustrates the typical cyclic voltammetry (CV) behavior of $O_2^{\cdot-}$ in DMF/0.1 M $Bu_4NBF_4$ within the potential window of 0.0 to -1.6 V at a glassy carbon electrode. The CV profiles depict the redox couple of free $O_2/O_2^{\cdot-}$ with one oxidation peak at -0.7 V and one reduction peak at -0.962 V. The impact of introducing a solution of 0.1 mM $TPPH_2$(o-methyl) and $TbPPH_2$ in the same solvent to the $O_2^{\cdot-}$ system is also demonstrated in Figure 4. The decrease in anodic peak current density, induced by the addition of $TPPH_2$(o-methyl) or $TbPPH_2$, is attributed to the reaction between $O_2^{\cdot-}$ and $TPPH_2$(o-methyl) or $TbPPH_2$ (Molyneux, 2004; Pisoschi *et al.*, 2009). This reduction serves as the basis for calculating the binding constant, while the shift in peak potential values aids in determining the mode of interaction (Milardović *et al.*, 2005; Milardovic *et al.*, 2006).

Upon adding 0.1 mM of $TPPH_2$(o-methyl) and $TbPPH_2$, a subtle positive shift in peak potential ΔE° is observed, accompanied by a noteworthy decrease in anodic peak current density. This phenomenon is linked to the scavenging activity of the added compounds (Sengul *et al.*, 2009). Table 3 summarizes the obtained results, highlighting the significant reduction in anodic peak current density attributed to the decline in $O_2^{\cdot-}$ radical concentration due to the formation of $O_2^{\cdot-}$_$TPPH_2$(o-methyl) and $O_2^{\cdot-}$_$TbPPH_2$ adducts.

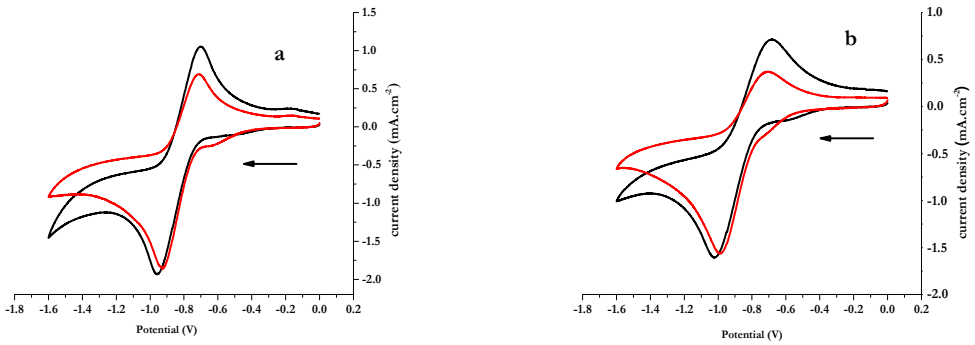


**Figure 4.** Cyclic voltammograms of oxygen-saturated DMF/0.1 $Bu_4NBF_4$ on a GC electrode in the absence (black line) and in presence of (red line) 0.1 mM of $TPPH_2$(o-methyl) (a) and $TbPPH_2$ (b), Scan rate 100 mV $s^{-1}$, T = 28 °C

The ratio of binding constants (Kox/Kred)

The observed positive shift in peak potential of the $O_2/O_2^{\cdot-}$ redox couple in the presence of $TPPH_2$(o-methyl) or $TbPPH_2$ suggests that the oxidation of $O_2^{\cdot-}$ becomes more facile in the presence of $TPPH_2$(o-methyl) or $TbPPH_2$. This phenomenon indicates that the oxidized form $O_2$ is more strongly bound to $TPPH_2$(o-methyl) or $TbPPH_2$ than its reduced form $O_2^{\cdot-}$ . For a system where both forms of the $O_2/O_2^{\cdot-}$ redox couple interact with $TPPH_2$(o-methyl) and $TbPPH_2$, Scheme 1 can be applied (Sengul *et al.*, 2009).

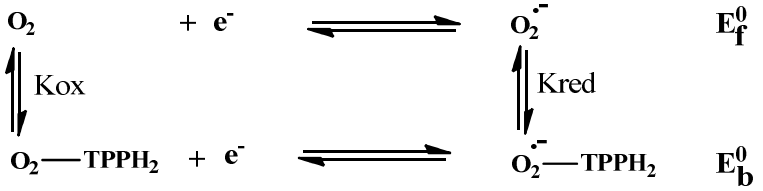


**Scheme 1.** Redox process of the free and $TPPH_2$ bound $O_2^{\cdot-}$ redox couple $TPPH_2$ represents $TPPH_2$(o-methyl) and $TbPPH_2$

The Nernst relationship applied to Scheme 1 leads to Equation (3) (Miller *et al.*, 1993):

$$\Delta E^0 = E_b^0 - E_f^0 = E^0\left(O_2^{\cdot-} - TPPH_2\right) - E^0\left(O_2^{\cdot-}\right) = 0.059\, log\, \frac{Kox}{Kred} \quad (3)$$

where $E_f^0$ and $E_b^0$ are the formal potentials of the $O_2/O_2^{\cdot-}$ couple in the free and bound forms, respectively. The decreasing rate of the anodic peak current density Δipa and the peak potential shift ΔE° are summarized in Table 3.

The ratio of the binding constants Kox/Kred is calculated by substituting ΔE° from Table 3 into Equation (3). The obtained ratios of the binding constants indicate that the interaction of the reduced form with $TPPH_2$(o-methyl) is 1.69 times higher than its oxidized form $O_2$, whereas the interaction of the reduced form $O_2^{\cdot-}$ with $TbPPH_2$ is 1.24 times stronger than the oxidized form $O_2$.

**Table 3.** Electrochemical data of the free and $O_2^{\cdot-}$ bound forms of $TPPH_2$(o-methyl) and $TbPPH_2$ used to calculate the ratio of the binding constants

| Compound | $Ep_a(V)$ | $Ep_c(V)$ | $E^0(V)$ | $\Delta E^0(mV)$ | $Kox/Kred$ |
|---|---|---|---|---|---|
| $O_2^{\cdot-}$ | -0.7 | -0.962 | -0.831 | - | - |
| $O_2^{\cdot-} - TPPH_2$(o-methyl) | -0.712 | -0.923 | -0.8175 | 13.5 | 1.69 |
| $O_2^{\cdot-}$ | -0.68 | -1.02 | -0.85 | - | - |
| $O_2^{\cdot-} - TbPPH_2$ | -0.708 | -0.981 | -0.8445 | 5.5 | 1.24 |

Binding constant

The introduction of varying concentrations of $TPPH_2$(o-methyl) and $TbPPH_2$ into a solution of DMF saturated with commercial oxygen results in a notable decrease in the peak current density, as depicted in Figure 5. This significant reduction in anodic peak current density is attributed to the decline in $O_2^{\cdot-}$ concentration due to the formation of $O_2^{\cdot-}\_TPPH_2$(o-methyl) and $O_2^{\cdot-}\_TbPPH_2$ products.

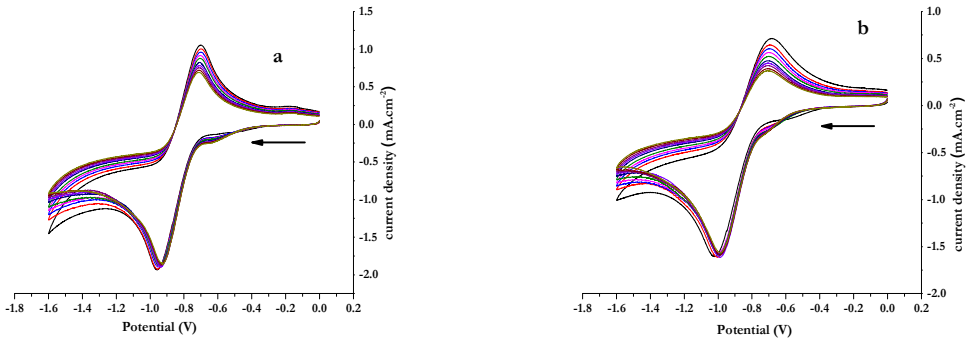


**Figure 5.** Cyclic voltammograms of oxygen-saturated DMF/0.1 $Bu_4NBF_4$ on a GC electrode in the absence and the presence of different concentrations of $TPPH_2$(o-methyl) (a) and $TbPPH_2$ (b), scan rate 100 mV/s, T = 28 °C

The gradual decrease in peak current density of the $O_2/O_2^{\cdot-}$ redox along with an increase of $TPPH_2$(o-methyl) and $TbPPH_2$ concentrations can be exploited to calculate the binding constant by applying equation (4) (Miller *et al.*, 1993),

$$log\frac{1}{C} = log\,K_b + log\frac{i}{i_0 - i} \quad (4)$$

Where C represents the concentration of $TPPH_2$(o-methyl) and $TbPPH_2$ (mol $L^{-1}$), $K_b$ refers to the binding constant (L $mol^{-1}$), and $i_0$ and i are the anodic peak current densities in the absence and presence of $TPPH_2$(o-methyl) and $TbPPH_2$, respectively. Figure 6 shows the plot of $log\frac{1}{C}$ versus $log\frac{i}{i_0 - i}$.

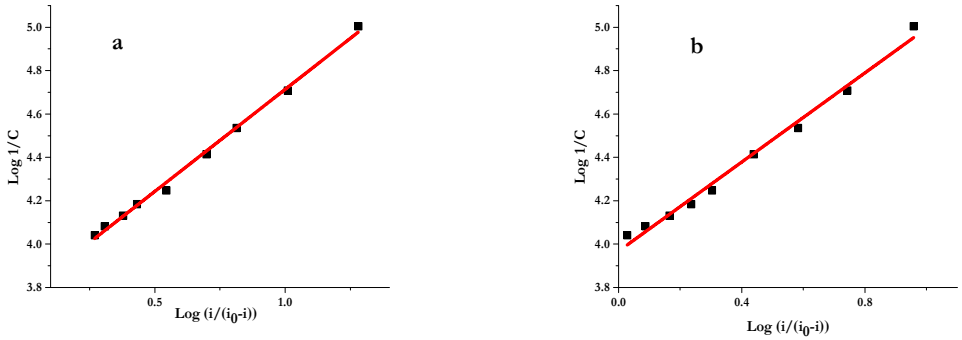


**Figure 6.** $log\frac{1}{C}$ versus $log\frac{i}{i_0 - i}$ for $O_2^{\cdot-}$ with varying concentration of $TPPH_2$(o-methyl) (a) and TbPPH2 (b) in DMF/0.1 $Bu_4NBF_4$, used to calculate the binding constants of $O_2^{\cdot-}$_$TPPH_2$(o-methyl) and $O_2^{\cdot-}$_$TbPPH_2$products

The intercept of the linear fitting of the plot $log\frac{1}{C}$ versus $log\frac{i}{i_0 - i}$ yielded the binding constants from which the binding free energy was calculated (Table 4).

The negative values of ΔG indicate the spontaneity of the $O_2^{\cdot-}$_$TPPH_2$(o-methyl) and $O_2^{\cdot-}$_$TbPPH_2$ interactions, whereas its magnitude indicates the weak binding between $O_2^{\cdot-}$ and $TPPH_2$(o-methyl) and $TbPPH_2$ (Gil *et al.*, 2002).

**Table 4.** Binding constants and binding free energies values of $O_2^{\cdot-}$_TPPH$_2$(o-methyl) and $O_2^{\cdot-}$_TbPPH$_2$products

| Compound | Equation | $R^2$ values | $K_b$ (L mol$^{-1}$) | -ΔG (kJ mol$^{-1}$) |
|---|---|---|---|---|
| TPPH2(o-methyl) | y = 0.941x + 3.773 | 0.996 | $5.92 \times 10^3$ | 21.54 |
| TbPPH2 | y = 1.028x + 3.967 | 0.988 | $9.27 \times 10^3$ | 22.65 |
| α-Tocopherol | y = 0.841x + 2.298 | 0.986 | $1.98 \times 10^2$ | 13.11 |

Diffusion coefficients

To determine the diffusion coefficients of the free radical $O_2^{\cdot-}$ and its bound forms $O_2^{\cdot-}$_TPPH$_2$(o-methyl) and $O_2^{\cdot-}$_TbPPH$_2$, voltammograms were collected by altering the potential scan rates, as illustrated in Figure 7. All the voltammograms exhibit distinct and stable redox peaks, indicative of the redox process of the $O_2/O_2^{\cdot-}$ couple.

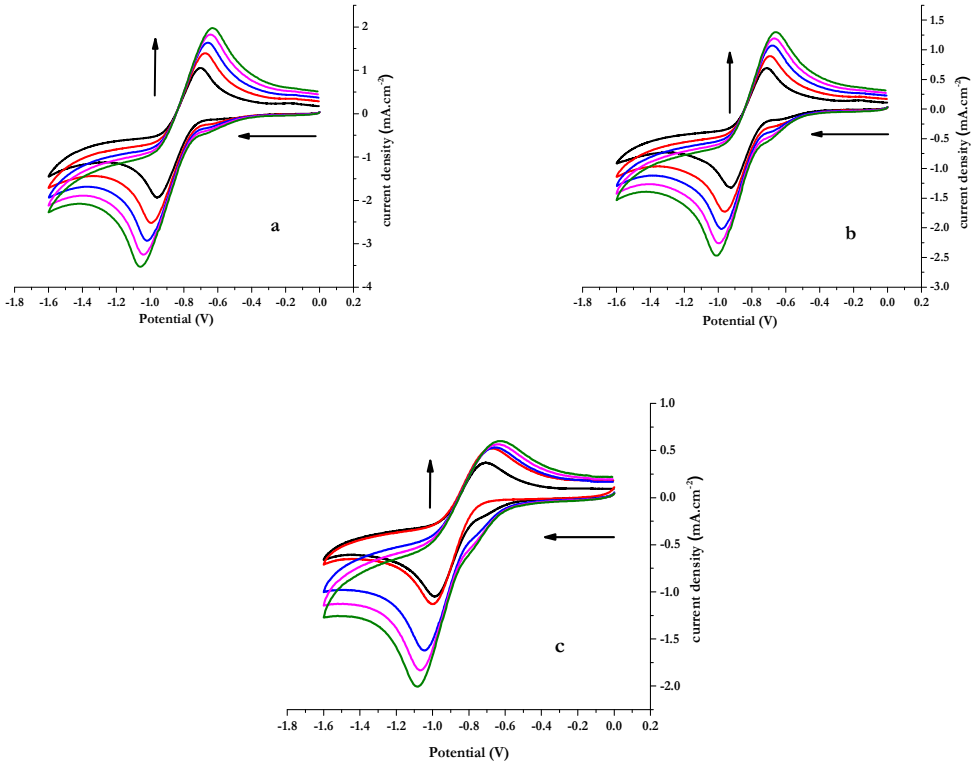


**Figure 7.** Succession of cyclic voltammograms at the GC electrode of free radical $O_2^{\cdot-}$ (a) and 90.91 µM of $O_2^{\cdot-}$_TPPH$_2$(o-methyl) (b) and $O_2^{\cdot-}$_TbPPH$_2$ (c) in oxygen-saturated DMF/0.1 $Bu_4NBF_4$ at various scan rates (100-500 mV, increment 100 mV) T = 28 °C. The vertical arrows indicate increasing scan rate

To further validate the interaction of $O_2^{\cdot-}$ radicals with TPPH$_2$(o-methyl) and TbPPH$_2$, the relationship ipa=f(v) was plotted before and after the addition of TPPH$_2$(o-methyl) and TbPPH$_2$ using Equation (5) (Brett *et al.*, 1993).

$$i = 2.69 \times 10^5 \left(\sqrt{n}\right)^3 SC\sqrt{D}\sqrt{v} \quad (5)$$

where i is the peak current (A), S is the surface area of the electrode (cm$^2$), C is the bulk concentration (mol.cm$^{-3}$) of the electroactive species, D is the diffusion coefficient (cm$^2$ s$^{-1}$), and v is the potential scan rate (V s$^{-1}$).

The linear dependence of the peak current density for both $O_2^{\cdot-}$ and the bound forms $O_2^{\cdot-}$_TPPH$_2$(o-methyl) and $O_2^{\cdot-}$_TbPPH$_2$ on the square root of the potential scan rates suggests that the redox process is kinetically controlled by the diffusion step, as illustrated in Figure 8.

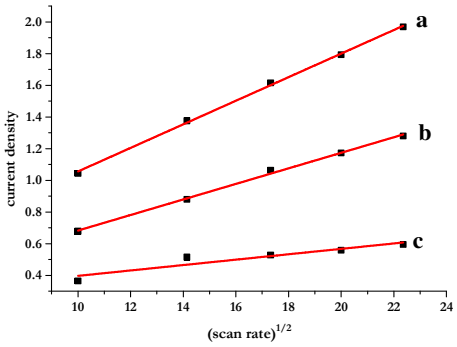


**Figure 8.** $ip_a$ vs $\sqrt{v}$ plots of oxygen-saturated DMF/0.1 $Bu_4NBF_4$ (a) in the presence of 90.91 µM of $TPPH_2$(o-methyl) (b), $TbPPH_2$ (c), at different scan rates under the experimental conditions of Figure 7

The diffusion coefficients of both free $O_2^{\cdot-}$ and bound forms $O_2^{\cdot-}$_TPPH$_2$(o-methyl) and $O_2^{\cdot-}$_TbPPH$_2$ were determined from the slopes of Randles-Sevcik plots, and the values are summarized in Table 5. The diffusion coefficients of bound $O_2^{\cdot-}$_TPPH$_2$(o-methyl) and $O_2^{\cdot-}$_TbPPH$_2$ are comparatively small when compared to free $O_2^{\cdot-}$, suggesting the formation of $O_2^{\cdot-}$_TPPH$_2$(o-methyl) and $O_2^{\cdot-}$_TbPPH$_2$ products. The decrease in the diffusion coefficient of $O_2^{\cdot-}$, in the presence of $TPPH_2$(o-methyl) and $TbPPH_2$ is attributed to the higher molecular weight of the formed products. The values are provided in Table 5.

**Table 5.** Diffusion coefficients values of free and $O_2^{\cdot-}$ bound $TPPH_2$(o-methyl) and $TbPPH_2$

| Compound | Equation | $R^2$ values | D ($cm^2 s^{-1}$) |
|---|---|---|---|
| $O_2^{\cdot-}$ | y = 0.074x + 0.312 | 0.999 | $4.53 \times 10^{-4}$ |
| $O_2^{\cdot-}$_TPPH$_2$(o-methyl) | y = 0.049x + 0.192 | 0.999 | $1.97 \times 10^{-4}$ |
| $O_2^{\cdot-}$_TbPPH$_2$ | y = 0.017x + 0.226 | 0.941 | $2.38 \times 10^{-5}$ |

*Homogeneous kinetics*

To calculate the second-order homogeneous rate constant (K) for the kinetics of free-radical scavenging, the pseudo-first-order rate constants ($K_f$) for the reaction of the studied antioxidant compounds and superoxide radical were first determined using the Nicholson-Shain equation (6) (Nicholson *et al.*, 1964).

$$E_{pa} = E_0 - \frac{RT}{nF}\left[\left(0.78 - ln\sqrt{\frac{nFK_f}{RTv}}\right)\right] \quad (6)$$

where $E_0$ is the formal potential of the $O_2/O_2^{\cdot-}$ redox couple in the free form, $E_{pa}$ is the anodic peak potential after the addition of the limit concentration of the studied antioxidant compounds, and v is the scan rate of the potential (mV $s^{-1}$).

Secondly, the values of the second-order homogeneous rate constant (K) for $TPPH_2$(o-methyl) and $TbPPH_2$ were determined using Equation (7) (Muhammad *et al.*, 2018).

$$K = \frac{K_f}{C} \quad (7)$$

where C is the limit concentration of the studied antioxidant compounds that allows obtaining the pseudo-first-order condition.

From the K values, the Gibbs energy of activation ($\Delta G^*$) was calculated using the following relation (Nicholson *et al.*, 1964; Muhammad *et al.*, 2018):

$$\Delta G^* = RT\, ln\frac{kT}{hK} \quad (8)$$

where k represents the Boltzmann constant, R is the gas constant, and $h$ is Planck's constant. The calculated values are presented in Table 6.

**Table 6.** Homogeneous rate constant and energy of activation for $TPPH_2$(o-methyl), $TbPPH_2$ and $\alpha$-tocopherol

| Entry | K ($M^{-1}\ S^{-1}$) | $\Delta G^*$ (kJ $mol^{-1}$) |
|---|---|---|
| $TPPH_2$(o-methyl) | 11.71 | 128.5 |
| $TbPPH_2$ | 10.01 | 147.7 |
| $\alpha$-tocopherol | 1.6 | 75.8 |

*Molecular docking study*

A comprehensive study employing molecular docking was conducted to elucidate the binding parameters and inhibition of $O_2^{\cdot-}$_$TPPH_2$(o-methyl) and $O_2^{\cdot-}$_$TbPPH_2$ with the enzyme glutathione reductase (GR). Glutathione reductase, also known as glutathione-disulfide reductase, is an enzyme that catalyzes the conversion of glutathione disulfide (GSSG) to reduced glutathione (GSH). GSH plays a crucial role in eliminating reactive oxygen species and acts as a scavenger for various oxygen radicals. The enzymatic reaction is represented by equation (9):

$$2GHS + NAPD^+ \leftrightarrow GSSG + NAPDH + H^+ \quad (9)$$

Inhibition of glutathione reductase results in a decrease in the level of reduced glutathione (GSH) and an increase in the level of glutathione disulfide (GSSG). Nicotinamide adenine dinucleotide phosphate (NADPH) is crucial for regenerating glutathione, and this process is essential for resisting oxidative stress and maintaining intracellular pH (Darraji *et al.*, 2022; Rasheed *et al.*, 2023). Therefore, studying the inhibition of glutathione reductase is a valuable approach for identifying potential antioxidants. An effective antioxidant candidate should reduce the inhibition of the glutathione reductase enzyme.

Molecular docking models, employing a rigid receptor and flexible ligand, were utilized to examine the inhibition of glutathione reductase by $O_2^{\cdot-}$_$TPPH_2$(o-methyl) and $O_2^{\cdot-}$_$TbPPH_2$ and to assess the strength of the interactions between them.

Results from the molecular docking indicate that hydrogen bonding, hydrophobic forces, and π-cation interactions contribute to the binding process. Figure 9 illustrates the interactions of compounds $O_2^{\cdot-}$_$TPPH_2$(o-methyl) and $O_2^{\cdot-}$_$TbPPH_2$, and alpha-tocopherol with nearby residues in the active site of glutathione reductase. The interacting residues, along with their corresponding bond types and lengths, are summarized in Table 7.

**Table 7.** Interaction types between ligands $O_2^{\cdot-}$_$TPPH_2$(o-methyl), $O_2^{\cdot-}$_$TbPPH_2$, alpha-tocopherol and glutathione reductase

| Molecule | Bond type | Amino acid (number of bonds/interactions) | Distance, Å |
|---|---|---|---|
| $O_2^{\cdot-}$_$TPPH_2$(o-methyl) | H-bonds | HIS52 | 3.75 |
| | Hydrophobic interactions | HIS52, VAL61, THR156, ASP178, ASP297, LEU298 (2) | 3.63, 3.65, 3.86, 3.93, 3.66, 3.32, 2.97 |
| | π-Stacking interactions | HIS52 | 4.19 |
| $O_2^{\cdot-}$_$TbPPH_2$ | H-bonds | HIS52 | 3.57 |

| | | | |
|---|---|---|---|
| | Hydrophobic interactions | HIS52, ASN60, VAL61, PRO65, VAL107 (2), THR176, GLN182 | 3.41, 3.64, 3.45, 3.52, 3.77, 3.30, 3.19, 3.37 |
| | π-Stacking interactions | HIS52 | 3.57 |
| alpha-tocopherol | H-bonds | LYS66 | 3.66 |
| | Hydrophobic interactions | LYS66, TYR197, LEU338, PRO368 (2), THR369, VAL370 (2), PHE372, GLN445 | 3.80, 3.47, 3.27, 3.45, 3.74, 3.15, 3.78, 3.41, 3.54, 3.47 |

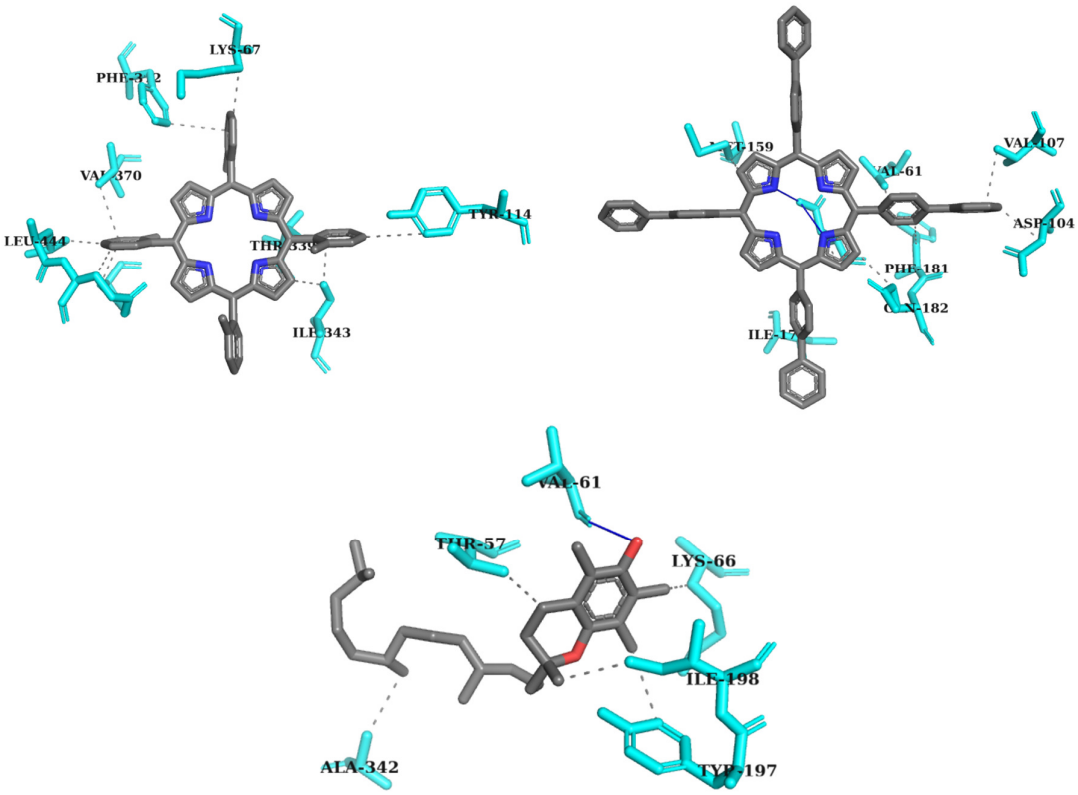


**Figure 9.** Best docking poses for glutathione reductase interacting with $O_2^{\cdot-}$_TPPH$_2$(o-methyl), $O_2^{\cdot-}$_TbPPH$_2$ and alpha-tocopherol illustrating H-bonds, hydrophobic, and π-stacking interactions

The table reveals that, apart from hydrophobic interactions, all compounds formed with glutathione reductase (GR) have only one hydrogen bond. The binding free energy and inhibitory concentration obtained from the molecular docking study for the compounds $O_2^{\cdot-}$_TPPH$_2$(o-methyl) and $O_2^{\cdot-}$_TbPPH$_2$, and alpha-tocopherol are summarized in Table 8.

**Table 8.** Binding free energies and inhibitory concentration obtained from molecular docking study

| Adduct | $O_2^{\cdot-}$_TPPH$_2$(o-methyl) | $O_2^{\cdot-}$_TbPPH$_2$ | alpha-tocopherol |
|---|---|---|---|
| ΔG (kJ mol$^{-1}$) | -7.019 | -8.459 | -8.019 |
| IC$_{50}$ (μM) | 7.09 | 0.63 | 1.31 |

Based on the robust results obtained from our antioxidant study and molecular docking simulations, it is compellingly evident that TbPPH$_2$ exhibits remarkable antioxidant properties. The compound demonstrated not only the highest antioxidant activities but also the lowest binding free energy, indicative of

its strong interaction with the target enzyme, glutathione reductase. Despite possessing a weaker binding affinity towards glutathione reductase compared to $TPPH_2$ (o-methyl) and alpha-tocopherol, $TbPPH_2$ still exhibited a substantially high inhibitory concentration of 0.63 µM against the enzyme reaction.

Moreover, molecular docking studies have gained increasing popularity in predicting ligand-protein interactions accurately. The utilization of molecular docking simulations in our study further strengthens the reliability of our results, providing valuable insights into the molecular mechanisms underlying the antioxidant activity of $TbPPH_2$.

Our findings align with previous studies that have investigated the antioxidant potential of porphyrin-based compounds. For instance, Boutarfaia *et al*. (2019; 2020). reported similar trends in antioxidant activity, highlighting the promising role of porphyrins in combating oxidative stress-related disorders. Additionally, recent works by Ahmed *et al*. (2020). and Abu-Melha *et al*. (2019). corroborate our findings, emphasizing the importance of exploring novel antioxidants for therapeutic interventions.

Docking validation

The docking procedure was validated by redocking of the co-crystalized ligand (FLAVIN-ADENINE DINUCLEOTIDE) to the binding site of glutathione reductase using the same methodology that was used previously in the docking process. The ligand was separated from the protein structure and saved as a pdb file. Water molecules and co-factors, which did not affect the binding site, were removed. Hydrogen atoms were added. The ligand was then re-docked into the active site using the same protocol including the grid parameters. The re-docked complex was then superimposed on to the reference co-crystallized complex, Figure 10 presents a superimposed view of the re-docked conformation (purple colour) and the original ligand (green colour), and the RMSD value between them is 0.9792 Å. The clear superimposed between both ligands and also the RMSD value less than 2 indicates the efficiency of the AutoDock algorithms to perform molecular docking protocol with confidence.

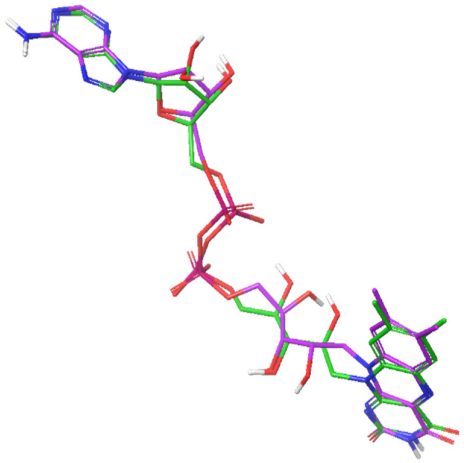

**Figure 10.** Comparison between the re-docked pose and original ligand; (purple: docked pose; green: original ligand) with an RMSD value of 0.9792 Å

ADME study

*In silico* ADME study was carried out to predict the adverse metabolic effects of oral administration of $TPPH_2$ (o-methyl) and $TbPPH_2$ as drug candidate, as well as their half-life in the organism and excretion route (Silvino *et al.*, 2016). Cytochrome P450 isoenzymes (CYP450) are oxidases that interact with drugs in order to decrease their plasma concentration and reduce the risks of toxicity by metabolic activation (Al-Darraji *et al.*, 2022; Rasheed *et al.*, 2023), as well as making them more water soluble for elimination (Eitrich *et al.*, 2007;

LANEZ *et al.*, 2023). Thus, a drug candidate should not inhibit cytochrome CYP450 isoenzymes because inhibition may increase the plasma concentration (Zahno *et al.*, 2011; Terkeltaub *et al.*, 2011).

Table 9 shows that both the studied porphyrins derivatives $TPPH_2$(o-methyl) and $TbPPH_2$ and the standard alpha-tocopherol are not inhibitors of CYP450 IA2, 2C19, 2C9, 2D6, 3A4 isoenzymes which suggests a decrease in their plasma concentrations and a rapid elimination route.

**Table 9.** Metabolism and excretion by the CYP450 isoenzymes inhibition of the $O_2^{\cdot-}$_$TPPH_2$(o-methyl) and $O_2^{\cdot-}$_$TbPPH_2$ and the standard alpha-tocopherol

| Compound | IA2 | 2C19 | 2C9 | 2D6 | 3A4 |
|---|---|---|---|---|---|
| $TPPH_2$(o-methyl) | No | No | No | No | No |
| $TbPPH_2$ | No | No | No | No | No |
| alpha-tocopherol | No | No | No | No | No |

The absence of metabolic interactions between $TPPH_2$(o-methyl), $TbPPH_2$, and alpha-tocopherol with key cytochrome P450 enzymes suggests a favorable safety profile regarding drug metabolism. These findings provide valuable insights for further exploration of these compounds in both preclinical and clinical settings. However, comprehensive in vivo studies are warranted to confirm these predictions and ensure the safe and effective use of these compounds in therapeutic applications. Additionally, considering the dynamic nature of drug metabolism, ongoing monitoring of potential interactions with other metabolic pathways is recommended to mitigate any unforeseen adverse effects.

## Conclusions

This study conducted both *in vitro* and *in silico* evaluations to assess the scavenging activity against $O_2^{\cdot-}$ and the antioxidant activity of two novel compounds: meso-tetramethophenyl-porphyrin ($TPPH_2$(o-methyl)) and meso-tetrabiphenyl-porphyrin ($TbPPH_2$). Cyclic voltammetry assays were employed to measure the decrease in anodic peak current density, providing insights into the binding parameters of the interaction of $O_2^{\cdot-}$ with $TPPH_2$(o-methyl) and $TbPPH_2$.

The systematic decrease in anodic peak current density with increasing concentrations of $TPPH_2$(o-methyl) and $TbPPH_2$ indicated strong interactions with the $O_2^{\cdot-}$ radicals, attributing antiradical activity to the added compounds. The $IC_{50}$ values, antioxidant activity coefficients, and binding constants suggested comparable antiradical activity and binding affinity for both compounds. Negative values of binding free energy indicated spontaneous and electrostatic interactions dominating the binding of $O_2^{\cdot-}$ with $TPPH_2$(o-methyl) and $TbPPH_2$.

Evaluation of diffusion coefficients using the Randles-Sevcik equation highlighted the slower diffusion of the bounded $O_2^{\cdot-}$_$TPPH_2$(o-methyl) and $O_2^{\cdot-}$_$TbPPH_2$ compared to free $O_2^{\cdot-}$ radical, indicating the formation of a slower-diffusing product.

Molecular docking studies revealed that meso-tetrabiphenyl-porphyrin ($TbPPH_2$) exhibited more inhibitory activity against glutathione reductase enzyme, with an inhibitory concentration of 0.63 μM and a docking score of -35.36 kJ/mol, making it the most promising antioxidant candidate. The congruence between in vitro and in silico results provides valuable insights for designing novel antioxidant porphyrin derivatives with reduced activity against glutathione reductase.

## Authors' Contributions

LZ: Data curation, Formal analysis, Funding acquisition, Methodology. LB: Investigation, Supervision, Resources, Software. EL: Writing - original draft, Validation, Visualization. TL: Project administration. All authors read and approved the final manuscript.

**Ethical approval** (for researches involving animals or humans)

Not applicable.

## Acknowledgements

The authors are grateful to the Ministry of Higher Education and Scientific research for the financial support of the project (B00L01UN390120110001). We also acknowledge the assistance of M. Ali Tliba from Laboratoire de Valorisation et Technologie des Ressources Sahariennes (VTRS) staff.

The authors also would like to thank Dr *NESBA Kaouther*, a doctor of Linguistics, for her assistance in proofreading the manuscript language.

## Conflict of Interests

The authors declare that there are no conflicts of interest related to this article.

## References

Abu-Melha S (2019). Efficient synthesis of meso-substituted porphyrins and molecular docking as potential new antioxidant and cytotoxicity agents. Archiv der Pharmazie 352(2). *https://doi.org/10.1002/ardp.201800221*

Ahmed A, Omar WAE, El-Asmy HA, Abou-Zeid L, Fadda AA (2020). Docking studies, antitumor and antioxidant evaluation of newly synthesized porphyrin and metalloporphyrin derivatives. Dyes and Pigments 183. *https://doi.org/10.1016/j.dyepig.2020.108728*

Ahmed S, Shakeel F (2012a). Antioxidant activity coefficient, mechanism, and kinetics of different derivatives of flavones and flavanones towards superoxide radical. Czech Journal of Food Sciences 30(2):153-163. *https://doi.org/10.17221/447/2010-cjfs*

Ahmed S, Shakeel F (2012b). Voltammetric determination of antioxidant character in *Berberis lycium* Royel, *Zanthoxylum armatum* and *Morus nigra* Linn plants. Pakistan Journal of Pharmaceutical Sciences 25(3):501-507. *https://www.pjps.pk/uploads/pdfs/CD-PJPS-25-3-12/Paper-2.pdf*

Al-Darraji MN, Jasim SA, Aldeen ODAS, Ghasemian A, Rasheed M (2022). The effect of LL37 antimicrobial peptide on FOXE1 and lncRNA PTCSC 2 genes expression in colorectal cancer (CRC) and normal cells. Asian Pacific Journal of Cancer Prevention 23(10):3437-3442. *https://doi.org/10.31557/APJCP.2022.23.10.3437*

Al-Darraji MN, Saqban LH, Rasheed M, Hussein AJ, Mutar TF (2022). Association of candidate genes polymorphisms in Iraqi patients with chronic kidney disease. Journal of Advanced Biotechnology and Experimental Therapeutics 5(3):687-701. *https://doi.org/10.5455/jabet.2022.d147*

Antolovich M, Prenzler PD, Patsalides E, McDonald S, Robards K (2002). Erratum: Methods for testing antioxidant activity. Analyst 127(3):430. *https://doi.org/10.1039/B009171P*

Boutarfaia A, Bechki L, Lanez T, Lanez E, Kadri M (2019a). Synthesis, antioxidant activity, and determination of binding parameters of Meso-Tetra-4-Actophenyl-Porphyrin and its Palladium (II) complex with superoxide anion

radicals. Current Bioactive Compounds 16(7):1063-1071. *https://doi.org/10.2174/1573407215666191017105239*

Boutarfaia A, Bechki L, Lanez T, Lanez E, Kadri M (2019b). Synthesis, antioxidant activity, and determination of binding parameters of Meso-Tetra-4-Actophenyl-Porphyrin and its Palladium (II) complex with superoxide anion radicals. Current Bioactive Compounds 16(7):1063-1071. *https://doi.org/10.2174/1573407215666191017105239*

Brand-Williams W, Cuvelier ME, Berset C (1995). Use of a free radical method to evaluate antioxidant activity. LWT - Food Science and Technology 28(1):25-30. *https://doi.org/10.1016/S0023-6438(95)80008-5*

Brett C, Oliveira Brett AM (1993). Electrochemistry: principles, methods, and applications. Electrochemistry 67(2):444. *https://cir.nii.ac.jp/crid/1130282271129959296*

Eitrich T, Kless A, Druska C, Meyer W, Grotendorst J (2007). Classification of highly unbalanced CYP450 data of drugs using cost sensitive machine learning techniques. Journal of Chemical Information and Modeling 47(1):92-103. *https://doi.org/10.1021/ci6002619*

Frisch MJ, Trucks GW, Schlegel HB, Scuseria GE, Robb MA, Cheeseman JR (2009). Gaussian 09. Wallingford, CT: Gaussian. *http://dx.doi.org/10.1007/978-1-4684-7424-4*

Gil MI, Tomás-Barberán FA, Hess-Pierce B, Kader AA (2002). Antioxidant capacities, phenolic compounds, carotenoids, and vitamin C contents of nectarine, peach, and plum cultivars from California. Journal of Agricultural and Food Chemistry 50(17):4976-4982. *https://doi.org/10.1021/jf020136b*

Giustarini D, Dalle-Donne I, Tsikas D, Rossi R (2009). Oxidative stress and human diseases: Origin, link, measurement, mechanisms, and biomarkers. Critical Reviews in Clinical Laboratory Sciences 46(5-6):241-81. *https://doi.org/10.3109/10408360903142326*

Ighodaro OM, Akinloye OA (2018). First line defence antioxidants-superoxide dismutase (SOD), catalase (CAT) and glutathione peroxidase (GPX): Their fundamental role in the entire antioxidant defence grid. Alexandria Journal of Medicine 54(4):287-293. *https://doi.org/10.1016/j.ajme.2017.09.001*

Karplus PA, Schulz GE (1989). Substrate binding and catalysis by glutathione reductase as derived from refined enzyme: Substrate crystal structures at 2Å resolution. Journal of Molecular Biology 210(1):163-180. *https://doi.org/10.1016/0022-2836(89)90298-2*

Kedadra A, Lanez T, Lanez E, Hemmami H, Henni M (2022). Synthesis and antioxidant activity of six novel N-ferrocenylmethyl-N-(nitrophenyl)and-N-(cyanophenyl)-acetamides: Cyclic voltammetry and molecular docking studies. Journal of Electrochemical Science and Engineering 12(2):293-304. *https://doi.org/10.5599/jese.1162*

Khennoufa A, Bechki L, Lanez T, Lanez E, Zegheb N (2021). Spectrophotometric, voltammetric and molecular docking studies of binding interaction of N-ferrocenylmethylnitroanilines with bovine serum albumin. Journal of Molecular Structure 1224. *https://doi.org/10.1016/j.molstruc.2020.129052*

Kim S, Thiessen PA, Bolton EE, Chen J, Fu G, Gindulyte A, *et al.* (2016). PubChem substance and compound databases. Nucleic Acids Research 44(D1):D1202-1213. *https://doi.org/10.1093/nar/gkv951*

Korotkova EI, Karbainov YA, Avramchik OA (2003). Investigation of antioxidant and catalytic properties of some biologically active substances by voltammetry. Analytical and Bioanalytical Chemistry 375(3):465-468. *https://doi.org/10.1007/s00216-002-1687-y*

Lanez E, Bechki L, Lanez T (2019a). Antioxidant Activities, Binding Parameters, and Electrochemical Behavior of Superoxide Anion Radicals Twords 1-Ferrocenylmethylthymine and 1-Ferrocenylmethylcytosine. Current Physical Chemistry 10(1):10-22. *https://doi.org/10.2174/1877946809666190424143752*

Lanez E, Bechki L, Lanez T (2019b). Computational molecular docking, voltammetric and spectroscopic DNA interaction studies of 9N-(Ferrocenylmethyl)adenine. Chemistry and Chemical Technology 13(1):11-17. *https://doi.org/10.23939/chcht13.01.011*

Lanez E, Zegheb N, Lanez T (2023). In silico ADME, toxicological analysis, molecular docking studies and Molecular dynamics simulation of Afzelin with potential antibacterial effects against Staphylococcus aureus. Turkish Computational and Theoretical Chemistry 7(3):10-16. *https://doi.org/10.33435/TCANDTC.1196422*

Lanez T, Hemmami H (2016). Antioxidant activities of N-ferrocenylmethyl-2- and -3-nitroaniline and determination of their binding parameters with superoxide anion radicals. Current Pharmaceutical Analysis 13(2):110-116. *https://doi.org/10.2174/1573412912666160831145524*

Lanez T, Henni M, Hemmami H (2015). Development of cyclic voltammetric method for the study of the interaction of antioxidant standards with superoxide anion radicals case of α-tocopherol. Scientific Study and Research: Chemistry and Chemical Engineering, Biotechnology, Food Industry 16(2):161-168. *https://pubs.ub.ro/dwnl.php?id=CSCC6201502V02S01A0006*

Laraoui H, Lanez E, Zegheb N, Adaika A, Lanez T, Benkhaled M (2023). Anti-diabetic activity of flavonol glucosides from *Fumana montana* Pomel: *In vitro* analysis, *in silico* docking, ADMET prediction, and molecular dynamics simulations. ChemistrySelect 8(8). *https://doi.org/10.1002/slct.202204512*

Li J, Fu A, Zhang L (2019). An overview of scoring functions used for protein–ligand interactions in molecular docking. Interdisciplinary Sciences – Computational Life Sciences 11(2):320-8. *https://doi.org/10.1007/s12539-019-00327-w*

Meraghni M, Lanez T, Lanez E, Bechki L, Kennoufa A (2023). Experimental and theoretical study on corrosion inhibition of mild steel by meso-tetraphenyl-porphyrin derivatives in acid solution. Journal of Electrochemical Science and Engineering 13(2):217-229. *https://doi.org/10.5599/jese.1400*

Milardović S, Iveković D, Grabarić BS (2006). A novel amperometric method for antioxidant activity determination using DPPH free radical. Bioelectrochemistry 68(2):175-180. *https://doi.org/10.1016/j.bioelechem.2005.06.005*

Milardovic S, Iveković D, Rumenjak V, Grabarić BS (2005). Use of DPPH•|DPPH redox couple for biamperometric determination of antioxidant activity. Electroanalysis 17(20):1847-1853. *https://doi.org/10.1002/elan.200503312*

Miller NJ, Rice-Evans C, Davies MJ, Gopinathan V, Milner A (1993). A novel method for measuring antioxidant capacity and its application to monitoring the antioxidant status in premature neonates. Clinical Science 84(4):407-412. *https://doi.org/10.1042/cs0840407*

Molyneux P (2004). The use of the stable free radical Diphenylpicryl-Hydrazyl (DPPH) for estimating antioxidant activity. Songklanakarin Journal of Science and Technology 26:211-219.

Morris GM, Goodsell DS, Halliday RS, Huey R, Hart WE, Belew RK, Olson AJ (1998). Automated docking using a Lamarckian genetic algorithm and an empirical binding free energy function. Journal of Computational Chemistry 19(14). *https://doi.org/10.1002/(SICI)1096-987X(19981115)19:14<1639::AID-JCC10>3.0.CO;2-B*

Morris GM, Huey R, Olson AJ (2008). UNIT using AutoDock for ligand-receptor docking. Current Protocols in Bioinformatics 24(24):8-14. *https://doi.org/10.1002/0471250953.bi0814s24*

Muhammad H, Hanif M, Tahiri IA, Versiani MA, Shah F, Khaliq O, ... Ahemd S (2018). Electrochemical behavior of superoxide anion radical towards quinones: a mechanistic approach. Research on Chemical Intermediates 44(10):6387-400. *https://doi.org/10.1007/s11164-018-3496-8*

Nicholson RS, Shain I (1964). Correction: Theory of stationary electrode polarography: single scan and cyclic methods applied to reversible, irreversible, and kinetic systems. Analytical Chemistry 36(7):1212. *https://doi.org/10.1021/ac60213a053*

Patra JK, Baek KH (2017). Green biosynthesis of magnetic iron oxide (Fe3O4) nanoparticles using the aqueous extracts of food processing wastes under photo-catalyzed condition and investigation of their antimicrobial and antioxidant activity. Journal of Photochemistry and Photobiology B: Biology 173:291-300. *https://doi.org/10.1016/j.jphotobiol.2017.05.045*

Pisoschi AM, Cheregi MC, Danet AF (2009). Total antioxidant capacity of some commercial fruit juices: Electrochemical and spectrophotometrical approaches. Molecules 14(1):480-93. *https://doi.org/10.3390/molecules14010480*

Rasheed M, Saleem MM, Marzoog TR, Taki MM, Bouras D, Hashim IA, ... Sarhan MA (2023). Effect of caffeine-loaded silver nanoparticles on minerals concentration and antibacterial activity in rats. Journal of Advanced Biotechnology and Experimental Therapeutics 6(2):495-509. *https://doi.org/10.5455/jabet.2023.d144*

Salentin S, Schreiber S, Haupt VJ, Adasme MF, Schroeder M (2015). PLIP: Fully automated protein-ligand interaction profiler. Nucleic Acids Research 43(W1):W443-447. *https://doi.org/10.1093/nar/gkv315*

Sen S, Chakraborty R, Sridhar C, Reddy YSR, De B (2010). Free radicals, antioxidants, diseases and phytomedicines: Current status and future prospect. International Journal of Pharmaceutical Sciences Review and Research 3(1):91-100.

Sengul M, Yildiz H, Gungor N, Cetin B, Eser Z, Ercisli S (2009). Total phenolic content, antioxidant and antimicrobial activities of some medicinal plants. Pakistan Journal of Pharmaceutical Sciences 22(1):102-6.

Silvino ACR, Costa GL, De Araújo FCF, Ascher DB, Pires DEV, Fontes CJF, ... Sousa TN (2016). Variation in Human Cytochrome P-450 drug-metabolism genes: A gateway to the understanding of plasmodium vivax relapses. PLoS One 11(7):e0160172. *https://doi.org/10.1371/journal.pone.0160172*

Steffen C, Thomas K, Huniar U, Hellweg A, Rubner O, Schroer A (2010). AutoDock4 and AutoDockTools4: automated docking with selective receptor flexibility. Journal of Computational Chemistry 31(16):2967-70. *https://doi.org/10.1002/jcc.21256*

Terkeltaub RA, Furst DE, Digiacinto JL, Kook KA, Davis MW (2011). Novel evidence-based colchicine dose-reduction algorithm to predict and prevent colchicine toxicity in the presence of cytochrome P450 3A4/P-glycoprotein inhibitors. Arthritis and Rheumatism 63(8):2226-2237. *https://doi.org/10.1002/art.30389*

Thompson SJ, Brennan MR, Lee SY, Dong G (2018). Synthesis and applications of rhodium porphyrin complexes. Chemical Society Reviews 47(3):929-981. *https://doi.org/10.1039/c7cs00582b*

Yao Y, Han X, Yang X, Zhao J, Chai C (2021). Detection of hydrazine at MXene/ZIF-8 nanocomposite modified electrode. Chinese Journal of Chemistry 39(2):330-336. *https://doi.org/10.1002/cjoc.202000398*

Zahno A, Brecht K, Morand R, Maseneni S, Török M, Lindinger PW, ... Krähenbühl S (2011). The role of CYP3A4 in amiodarone-associated toxicity on HepG2 cells. Biochemical Pharmacology 81(3):432-441. *https://doi.org/10.1016/j.bcp.2010.11.002*

Zaiz T, Lanez T (2015). Corrosion inhibition of carbon steel XC70 in $H_2SO_4$ solution by ferrocene derivative 3-(ferrocenylmethylamine)benzonitrile. Journal of Fundamental and Applied Sciences 4(2):182. *https://doi.org/10.4314/jfas.v4i2.8*

Zuriaga-Monroy C, Oviedo-Roa R, Montiel-Sánchez LE, Vega-Paz A, Marín-Cruz J, Martínez-Magadán JM (2016). Theoretical study of the aliphatic-chain length's electronic effect on the corrosion inhibition activity of methylimidazole-based ionic liquids. Industrial and Engineering Chemistry Research 55(12):3506-3516. *https://doi.org/10.1021/acs.iecr.5b03884*